

SLD-L2S: Hierarchical Subspace Latent Diffusion for High-Fidelity Lip to Speech Synthesis

Yifan Liang^{1,2}, Andong Li^{1,2}, Kang Yang³, Guochen Yu⁴, Fangkun Liu^{1,2}, Lingling Dai^{1,2}, Xiaodong Li^{1,2}, Chengshi Zheng^{1,2*}

¹Institute of Acoustics, Chinese Academy of Sciences, Beijing, China

²University of Chinese Academy of Sciences, Beijing, China

³School of Artificial Intelligence and Computer Science, Jiangnan University, Wuxi, China

⁴Zhipu AI

liangyifan@mail.ioa.ac.cn, liandong@mail.ioa.ac.cn, 6233110046@stu.jiangnan.edu.cn, guochen.yu@aminer.cn, liufangkun@mail.ioa.ac.cn, dailingling@mail.ioa.ac.cn, lxd@mail.ioa.ac.cn, cszheng@mail.ioa.ac.cn

Abstract

Although lip-to-speech synthesis (L2S) has achieved significant progress in recent years, current state-of-the-art methods typically rely on intermediate representations such as mel-spectrograms or discrete self-supervised learning (SSL) tokens. The potential of latent diffusion models (LDMs) in this task remains largely unexplored. In this paper, we introduce SLD-L2S, a novel L2S framework built upon a hierarchical subspace latent diffusion model. Our method aims to directly map visual lip movements to the continuous latent space of a pre-trained neural audio codec, thereby avoiding the information loss inherent in traditional intermediate representations. The core of our method is a hierarchical architecture that processes visual representations through multiple parallel subspaces, initiated by a subspace decomposition module. To efficiently enhance interactions within and between these subspaces, we design the diffusion convolution block (DiCB) as our network backbone. Furthermore, we employ a reparameterized flow matching technique to directly generate the target latent vectors. This enables a principled inclusion of speech language model (SLM) and semantic losses during training, moving beyond conventional flow matching objectives and improving synthesized speech quality. Our experiments show that SLD-L2S achieves state-of-the-art generation quality on multiple benchmark datasets, surpassing existing methods in both objective and subjective evaluations.

Introduction

Lip-to-speech (L2S) synthesis is the task of generating audible speech solely from visual lip movements (Milner and Le Cornu 2015), which presents potential for diverse applications, including automated video dubbing, robust communication in challenging acoustic environments, and assistive technologies for individuals with vocal impairments such as dysphonia and aphonia. The primary challenge in L2S synthesis lies in the ill-posed nature of mapping ambiguous visual cues to the complex acoustic features of speech. Traditional L2S methods (Prajwal et al. 2020; Wang and Zhao 2022; Kim, Kim, and Chung 2024) are largely confined to constrained settings, characterized by limited vocabularies

and speaker-dependent models, limiting their practicality in unconstrained and real-world scenarios.

Recent advances in self-supervised learning (SSL) (Hsu et al. 2021) and speech synthesis (Ren et al. 2020; Polyak et al. 2021) have catalyzed significant progress in L2S, enabling the generation of high-fidelity speech from corresponding visual inputs. The field has evolved from early, constrained settings (Cooke et al. 2006; Harte and Gillen 2015) to robust multi-speaker systems that perform effectively in unconstrained, real-world environments (Chung et al. 2017; Afouras, Chung, and Zisserman 2018). The integration of SSL has been particularly transformative, allowing models to learn rich semantic representations from vast unlabeled data. For instance, recent studies (Hsu et al. 2023; Choi, Kim, and Ro 2023) have leveraged powerful audio-visual SSL models like AV-HuBERT (Shi et al. 2022) to achieve significant gains in the intelligibility of synthesized speech. Concurrently, diffusion-based generative models (Défossez et al. 2022; Lipman et al. 2022) have emerged as a powerful paradigm for L2S synthesis, setting a new benchmark for synthesis quality (Choi, Hong, and Ro 2023; Yemini et al. 2023; Choi et al. 2025; Kim et al. 2025).

Despite significant progress, existing L2S methods predominantly rely on generating intermediate representations, such as mel-spectrograms or discrete SSL tokens. These representations, while effective for conveying semantic content, often fail to encapsulate the fine-grained acoustic details requisite for high-fidelity waveform generation. This limitation stems from two primary factors. First, the visual-to-audio mapping is an inherently ill-posed, one-to-many problem: a single lip movement sequence can correspond to multiple valid speech renderings with variations in prosody, emotion, and speaking style. Mel-spectrograms, as a physically-defined acoustic representation, lack the flexibility to model this diversity. Second, while discrete SSL tokens are potent for semantic representation, they are inherently coarse and may discard crucial acoustic details that are necessary for perceptual quality. Other approaches (Liang et al. 2025a,b) employ end-to-end training, bypassing explicit mapping strategies to prevent potential information loss. However, the resulting speech quality remains limited, suggesting that such methods necessitate high-quality large-scale audio-

*Corresponding author is Chengshi Zheng

Copyright © 2026, Association for the Advancement of Artificial Intelligence (www.aaai.org). All rights reserved.

visual datasets to retrain vocoder. These shortcomings motivates a central question: *Can we identify an alternative representation that more effectively captures the detailed acoustic characteristics required for high-fidelity L2S synthesis?*

Fortunately, latest progress in text-to-speech (TTS) synthesis (Wang et al. 2023; Du et al. 2024) have demonstrated the effectiveness of neural audio codecs (Zeghidour et al. 2021; Défossez et al. 2022), which learn to encode and decode audio waveforms into discrete latent representations. These codecs have shown remarkable performance in generating high-fidelity speech by capturing detailed acoustic characteristics. The success of these codecs in TTS tasks suggests that they are probably be beneficial for L2S synthesis. However, existing L2S methods have not yet fully explored the potential of audio codec latent vectors for L2S. While Uni-Dubing (Lei et al. 2024) has explored incorporating Hifi-Codec (Yang et al. 2023) to synthesis speech, it frames the problem as predicting multiple residual discrete tokens within a language modeling paradigm. This method presents significant challenges in L2S, because the limited visual input provides insufficient information to support a complicated language modeling task.

In this work, we present SLD-L2S, a novel L2S framework to generate high-fidelity speech directly from visual inputs using a hierarchical subspace latent diffusion model. A key component of our framework is the decomposition of visual representations into multiple subspaces to enable more robust cross-modal mapping. Initially, visual representations are extracted by a pre-trained visual encoder and subsequently processed by our proposed subspace decomposition module. To effectively model these decomposed representations, we introduce diffusion convolution block (DiCB) as the backbone of our generative model. Unlike diffusion transformer (DiT) architectures (Peebles and Xie 2023), our DiCB leverages the inductive biases of convolution to capture both temporal and cross-subspace dependencies. Furthermore, we employ a reparameterized flow matching (Lipman et al. 2022) objective to enable direct prediction of continuous latents. To enhance speech intelligibility, our training strategy extends beyond a standard flow matching loss by incorporating two auxiliary loss: a semantic consistency loss imposed on the latent vectors and a speech language model (SLM) loss evaluated on the final synthesized waveform. During the inference, the generated latent vectors are decoded into the final audio waveform by the pre-trained neural audio codec. Leveraging these architectural and methodological innovations, SLD-L2S achieves state-of-the-art results on benchmark datasets. The primary contributions of this work are summarized as follows:

- We propose a novel L2S framework for direct generation of the pre-trained audio codec latent vectors from visual inputs via a hierarchical subspace latent diffusion model.
- We design diffusion convolution blocks, subspace decomposition and recomposition modules to effectively map different modalities representations in subspaces.
- We introduce a reparameterized flow matching technique for direct latent vector generation to improve the generation quality in L2S.

Related Work

Multi-Speaker Lip to Speech Synthesis

Recent advances in deep learning have transformed L2S synthesis, driving the field from speaker-dependent models in constrained settings toward versatile multi-speaker systems. A pivotal development has been the integration of SSL techniques, which enhances performance by leveraging powerful semantic representations learned from vast unlabeled audio-visual data. For instance, recent studies (Hsu et al. 2023; Choi, Kim, and Ro 2023; Lei et al. 2024; Liang et al. 2025a) have effectively used pre-trained SSL models like AV-Hubert as potent feature extractors, yielding significant improvements in speech intelligibility. Concurrently, generative diffusion models have become a dominant paradigm. Early approaches in this domain, such as DiffV2S (Choi, Hong, and Ro 2023) and LipVoicer (Yemini et al. 2023), employed denoising diffusion probabilistic models (DDPMs) (Ho, Jain, and Abbeel 2020) to synthesize mel-spectrograms conditioned on visual features and auxiliary inputs like vision-guided speaker embeddings and semantic information from lip-reading models. More recent works, including V2SFlow (Choi et al. 2025) and From Faces to Voices (Kim et al. 2025) introduce flow matching (Lipman et al. 2022) to further advancing synthesis quality and demonstrating the remarkable potential of diffusion model for L2S.

Except generating intermediate representations like mel-spectrograms or discrete SSL tokens, Uni-Dubbing (Lei et al. 2024) has incorporated Hifi-Codec, which formulates the problem as predicting discrete residual tokens. This aligns with recent trends in TTS, where audio codecs are increasingly used to improve speech quality. However, the information-sparse visual modality provides constraints for the high-precision categorical prediction of discrete tokens. In contrast, our proposed SLD-L2S framework directly generates the latent vectors of a pre-trained audio codec from visual inputs, utilizing a hierarchical subspace latent diffusion model.

Neural Audio Codec

Neural audio codecs are a class of generative models engineered for high-fidelity audio compression (Zeghidour et al. 2021; Défossez et al. 2022; Kumar et al. 2023). Architecturally, they comprise an encoder that maps continuous raw waveforms into a sequence of discrete tokens, and a corresponding decoder that synthesizes a high-quality waveform from these tokens. The quantization of the output of encoder is typically achieved through residual vector quantization (RVQ). This method recursively quantizes the residual signal from previous quantization step, with each stage employing a distinct codebook to progressively capture more detail.

Beyond compression, the audio codecs have become instrumental in generative speech tasks. By repurposing the encoder of a pre-trained codec as acoustic tokenizers, speech synthesis can be reframed as a conditional sequence-to-sequence modeling problem, akin to tasks in natural language processing (NLP). A prominent example is VALL-E

(Wang et al. 2023), which auto-regressively predicts discrete acoustic tokens conditioned on textual and acoustic prompts. However, this token-prediction approach is ill-suited for L2S synthesis as previous discussions. Inspired by the approach in NaturalSpeech2 (Shen et al. 2023), which models the continuous latent space prior to quantization, we eschew the problematic discrete prediction task. Instead, our method is designed to directly generate the continuous latent vectors of a pre-trained audio codec conditioned on visual inputs.

Flow Matching

Flow matching (Lipman et al. 2022) has emerged as a powerful technique for generative modeling, garnering significant attention across diverse domains, including image (Esser et al. 2024), video (Zheng et al. 2024), and speech generation (Chen et al. 2024). Its efficacy in L2S synthesis has been demonstrated by recent works like V2SFLow (Choi et al. 2025) and From Faces to Voices (Kim et al. 2025). Specifically, V2SFLow achieves speech generation by generating speech through various acoustic attributes, while From Faces to Voices maps these attributes through a hierarchical visual encoder to enable L2S synthesis.

Given samples x_1 from a target data distribution and samples x_0 from a standard Gaussian, the core objective of flow matching is to learn a continuous vector field $v_\theta(x_t, t)$ that maps x_0 to x_1 along an ordinary differential equation (ODE) path defined as $dx_t = v_\theta(x_t, t)dt$. A common approach for training involves a simple linear flow, where the path is defined as

$$x_t = (1 - t)x_0 + tx_1, t \in [0, 1]. \quad (1)$$

For this specific linear path, the ground truth velocity field is analytically given by $v(x_t, t) = \frac{dx_t}{dt} = x_1 - x_0$. We can train a neural network v_θ to approximate this ground truth velocity at any continuous point x_t on the path from x_0 to x_1 at time $t \in [0, 1]$ by minimizing the following objective:

$$\mathbb{E}_{x_0 \sim p_0, x_1 \sim p_1, t} [||v_\theta(x_t, C, t) - (x_1 - x_0)||_2^2], \quad (2)$$

where C represents the context information guiding the generation process. In our specific case, C corresponds to the visual representations extracted from the input video frames.

During inference, to generate new samples from the target distribution, we start by sampling x_0 from the source distribution. Then, the sample x_t is iteratively updated using the learned velocity function $v_\theta(x_t, C, t)$ until it approximates x_1 at the target distribution. This process essentially solves the ODE using numerical methods, commonly the Euler method:

$$x_{t+1} = x_t + v_\theta(x_t, C, t)\Delta t, \quad (3)$$

where Δt is the step size. This iterative procedure enables sample generation from the target distribution by following the learned velocity field, which effectively guides samples from the source distribution.

Proposed Method

Overview

The overall architecture of our proposed L2S framework, SLD-L2S, is depicted in Figure 1. The central principle of

our approach is to learn a direct mapping from visual representations to the continuous latent space of a pre-trained neural audio codec. To achieve this, we employ a hierarchical subspace latent diffusion model that conditioned on visual representations through multiple parallel subspaces. Except traditional denoising loss, the entire framework is also optimized with a multi-level loss function, designed to ensure both the acoustic fidelity and the semantic consistency of the synthesized speech.

Visual Frontend

The visual frontend of our framework is responsible for extracting linguistic features from the input video sequence. To this end, we employ the visual frontend of AV-Hubert Large (Shi et al. 2022), a self-supervised audio-visual model pre-trained on the large-scale LRS3 (Afouras, Chung, and Zisserman 2018) and VoxCeleb2 (Chung, Nagrani, and Zisserman 2018) datasets. Consistent with prior work, we find AV-Hubert to be highly effective, as it provides visual representations that are rich in phonetic content, which is well-suited for L2S synthesis.

Hierarchical Subspace Latent Flowmatching

Subspace Decomposition The initial stage of our latent flow matching model involves decomposing the visual representation into a multi-subspace representation. First, the visual features extracted from the AV-Hubert encoder are temporally upsampled to match the resolution of the latent space of target audio codec. Subsequently, instead of a monolithic mapping, the upsampled features are channeled into a set of parallel convolutional subspaces. Each subspace, consisting of layer normalization and 1D convolution, is designed to learn a distinct subspace representation. These parallel subspace representations are then concatenated to form a unified tensor, which serves as the input to the DiCB backbone. Following standard practice in diffusion models (Peebles and Xie 2023), the time step t and speaker embedding c_s are projected via an adaptive layer norm (AdaLN) block to generate scale and shift parameters for conditional modulation within the network.

Diffusion Convolution Block The mapping from visual to acoustic features is a complex cross-modal transformation characterized by intricate, multi-scale dependencies. While transformer-based architectures like the DiT excel in many generative tasks, their monolithic self-attention mechanism can be sub-optimal for capturing the localized and hierarchical patterns inherent in this problem. To address this, we introduce the DiCB as the fundamental building block of our generative model. Drawing inspiration from both DiT and Conv2Former (Hou et al. 2024), DiCB is designed to efficiently process the decomposed subspace representations.

In a significant departure from DiT, we replace the standard self-attention and MLP layers with specialized convolutional modules, inheriting design principles from Conv2Former. This makes the DiCB architecture inherently insensitive to variations in sequence length, a desirable property for L2S applications. The core of each block is a convolutional attention module. Here, a depthwise convolution

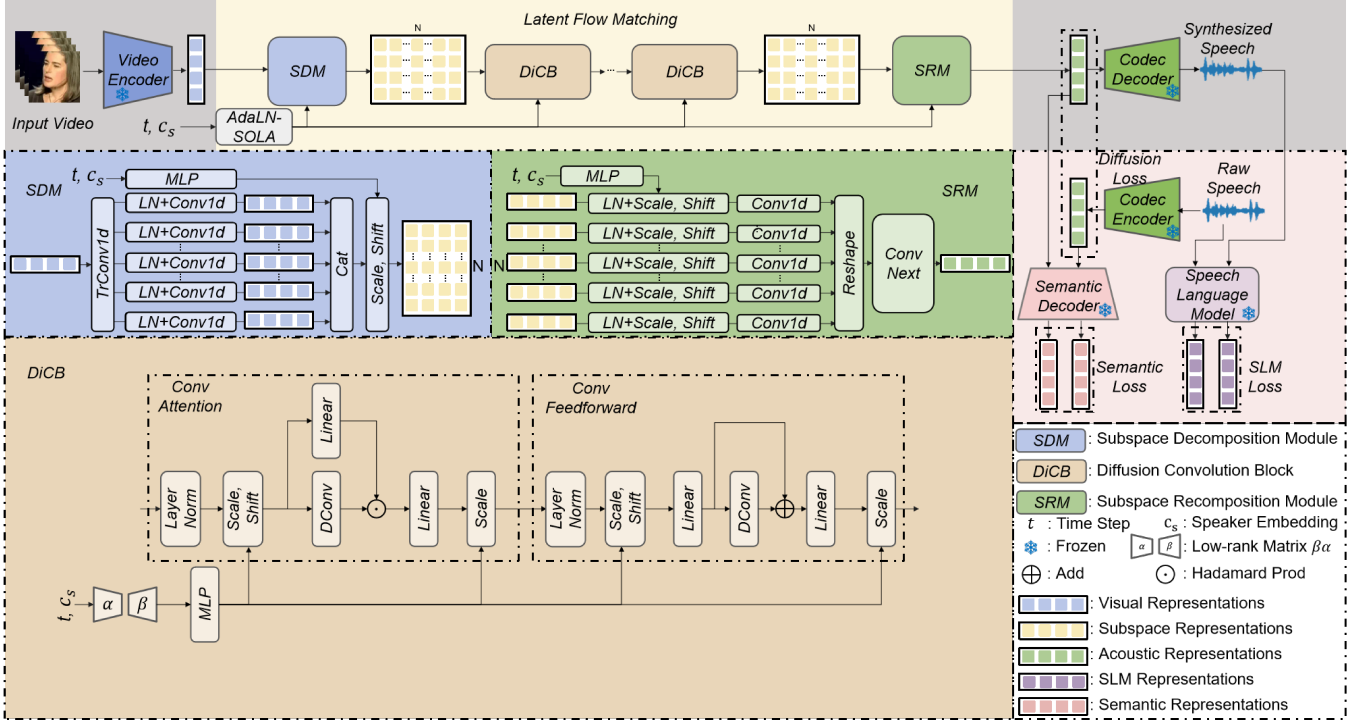


Figure 1: The model utilizes a latent flow matching approach to directly map visual features to the continuous acoustic latent space. The architecture consists of three main stages: a subspace decomposition module processes visual features into parallel pathways; a backbone of DiCBs, conditioned with AdaLN-SOLA, effectively refines these representations; and a subspace recomposition module fuses them into a final latent vector. The model is trained with a multi-objective function, including a flow matching loss for acoustic reconstruction, a semantic loss on the latent space, and an SLM loss on the final synthesized waveform. During inference, the model generates the latent vectors for the codec to synthesize into speech.

with a kernel size of $t \times k$ (where t and k are the kernel dimensions along time and subspace, respectively) is used to model local feature dependencies, and the output is produced via a Hadamard product with the value projection. This design efficiently models local and cross-subspace interactions. This is followed by a convolutional feedforward module, which facilitates channel-wise information mixing, analogous to the FFN in a standard transformer block.

Another key feature of DiCB is its conditioning mechanism. Similar to DiT, we integrate the time step t and speaker embedding c_s using an adaptive layer normalization module. Specifically, we employ AdaLN-SOLA (Hai et al. 2024), which reduces parameterization and computational overhead by using a single shared AdaLN module across all blocks and timesteps. Furthermore, it incorporates a low-rank adjustment mechanism to modulate the normalization parameters based on the conditioning variables, which we find stabilizes training and preserving performance.

Subspace Recomposition The final stage of our latent flow matching model, the subspace recomposition module, transforms the processed features from the DiCB backbone into the target latent space format of the audio codec. The output of the backbone, which now contains highly integrated feature representations, is first conditioned on the time step t and speaker embedding c_s using an AdaLN layer.

To address dimensional mismatch between DiCB outputs and the latent vectors of the audio codec, a 1D convolution and a reshape operation are applied to project the tensor to the correct output dimensions. Finally, we incorporate a ConvNeXt block (Liu et al. 2022) to ensure a robust fusion of information across the feature channels. This block enables high-order interactions and allows the model to learn an optimal combination of the multi-subspace features.

Training Objectives

Reparameterized Flow Matching Loss The standard Flow Matching objective seeks to estimate the velocity field v_θ by minimizing a mean squared error (MSE) loss, as defined in Eq. 2. However, this formulation can be unstable in our practice because it requires the network to regress a noise-dependent random derivative. The stochastic nature of this target prevents the use of auxiliary losses and complicates optimization. Inspired by (Fu et al. 2025), we adopt a reparameterized objective. Instead of directly predicting the velocity field v_θ , we reformulate the output of our model to be a direct estimate of the target data point, x_1 . This reparameterization not only improves training stability but also provides a more intuitive framework for incorporating auxiliary losses that operate in the data space. Specifically, we define the output of our model $d_\theta(x_t, c_s, t)$ as a direct pre-

Method	NFE	LRS3-TED						LRS2-BBC					
		UTMOS↑	SCOREQ↑	D-BERT↑	WER↓	SECS↑	UTMOS↑	SCOREQ↑	D-BERT↑	WER↓	SECS↑		
Ground Truth	–	3.5721	3.8105	–	0.71	–	3.0538	3.3008	–	1.35	–		
Intelligible	1	2.7019	2.7024	0.8231	27.73	0.761*	2.3315	2.3437	0.7932	36.50	0.701*		
DiffV2S	1000	3.0681	3.3811	0.7408	35.81	0.627	2.9575	3.2721	0.7103	47.58	0.569		
LipVoicer	400	2.4540	2.6598	0.7132	20.62	0.588	2.3756	2.7973	0.6906	24.92	0.578		
NaturalL2S	1	3.6598	3.7695	0.8068	30.37	0.628	3.5014	3.6702	0.7838	39.19	0.562		
V2SFlow	30	3.6939	4.0710	0.8306	27.55	0.851*	3.4556	3.9157	0.8064	34.17	0.820*		
Proposed	10	4.2096	4.6075	0.8284	30.22	0.804*	4.1664	4.5706	0.8005	39.54	0.756*		

Table 1: Lip-to-speech synthesis performance comparisons on LRS3-TED and LRS2-BBC dataset. \uparrow : higher is better, \downarrow : lower is better. The * indicates methods utilizing reference speaker embedding.

dition of the target sample x_1 . This relates to the velocity field v_θ via the linear probability path defined in Eq. 1:

$$d_\theta(x_t, c_s, t) = x_t + (1-t)v_\theta(x_t, c_s, t). \quad (4)$$

Consequently, the velocity field v_θ is learned implicitly. The reparameterized Flow Matching loss, \mathcal{L}_{FM} , is then formulated as a weighted MSE between the model’s prediction and the target x_1 :

$$\mathcal{L}_{FM} = \mathbb{E}_{x_0, x_1, t} \left[\frac{\|d_\theta(x_t, c_s, t) - x_1\|_2^2}{(1-t)^2} \right], \quad (5)$$

where $x_0 \sim p_0$, $x_1 \sim p_1$, and $t \sim U(0, 1)$.

Auxiliary Losses To improve the perceptual quality and content accuracy of the synthesized audio, we first incorporate SLM loss based on a pre-trained SLM. This SLM loss facilitates knowledge transfer by enforcing consistency in a high-level perceptual feature space. Specifically, we decode the predicted latent vector $d_\theta(x_t, c_s, t)$ and the target latent vector x_1 into waveforms using the audio codec’s decoder $D_a(\cdot)$. We then extract feature representations from both waveforms using the SLM and compute the squared L2 distance between them:

$$\mathcal{L}_{SLM} = \mathbb{E}_{x_0, x_1, t} \left[\|SLM(D_a(d_\theta(x_t, c_s, t))) - SLM(D_a(x_1))\|_2^2 \right], \quad (6)$$

Meanwhile, inspired by recent work on semantically-aware audio codecs like X-codec (Ye et al. 2025), we introduce a semantic loss to enforce content consistency directly at the latent level. This loss ensures that the generated codec latents retain the same core semantic content as the target latents. To achieve this, we use a separately pre-trained semantic decoder, $D_s(\cdot)$, which is trained in an auto-encoder setup (with a corresponding semantic encoder) to reconstruct semantic features (e.g., from HuBERT (Hsu et al. 2021) or WavLM (Chen et al. 2022)) from the codec latents. The semantic loss is the squared L2 distance between the reconstructed semantic features of the predicted and target latents:

$$\mathcal{L}_{sem} = \mathbb{E}_{x_0, x_1, t} \left[\|D_s(d_\theta(x_t, c_s, t)) - D_s(x_1)\|_2^2 \right], \quad (7)$$

where $D_s(\cdot)$ is the pre-trained semantic decoder, which is implemented as a multi-layer convolutional network.

The final training objective for our SLD-L2S framework is a weighted combination of these multi-objective losses:

$$\mathcal{L} = \mathcal{L}_{FM} + \lambda_1 \mathcal{L}_{SLM} + \lambda_2 \mathcal{L}_{sem}, \quad (8)$$

where λ_1 and λ_2 are hyperparameters balancing the contribution of each auxiliary objective. This multi-objective loss structure allows the model to jointly optimize for perceptual quality and semantic content, leading to improvements in overall synthesis performance.

Experimental Setup

Datasets

Our experiments are conducted on multi-speaker audio-visual benchmarks: LRS3-TED (Afouras, Chung, and Zisserman 2018) and LRS2-BBC (Chung et al. 2017). The LRS3-TED dataset, derived from TED and TEDx talks, contains approximately 439 hours of footage from over 5,000 speakers across 150,000 utterances. The LRS2-BBC dataset consists of 200 hours of data from BBC broadcasts, comprising 144,000 segments from a diverse set of speakers. We only use the LRS3-TED corpus for training, following its official pre-defined splits for training, validation, and testing. To assess the generalization capabilities of each method, we also evaluate on the LRS2-BBC test set.

Implementation Details

Our data pre-processing follows the pipeline in (Shi et al. 2022). For each video, we extract facial landmarks using the dlib (King 2009) library, crop the mouth region-of-interest (ROI), resize it to an 88x88 resolution and convert to grayscale. These frames are then processed by a pre-trained AV-Hubert Large model, which functions as our visual encoder, yielding 1024-dimensional feature vectors. For audio synthesis, we employ X-Codec-hubert as our neural audio codec, which operates at a 16 kHz sampling rate and was pre-trained on the LibriSpeech corpus. The speaker identity is provided via a 256-dimensional embedding c_s , extracted from a reference utterance using a GE2E (Wan et al. 2018). For our auxiliary losses, semantic features are extracted using a pre-trained HuBERT-base-Is960 model and we use WavLM (Chen et al. 2022) for calculating SLM loss. To

Method	Naturalness↑	Intelligibility↑	Similarity↑
Ground Truth	4.36 ± 0.15	4.48 ± 0.15	—
Intelligible	2.82 ± 0.25	3.37 ± 0.26	3.02 ± 0.17
DiffV2S	2.95 ± 0.27	2.98 ± 0.27	2.80 ± 0.23
LipVoicer	2.51 ± 0.23	2.97 ± 0.29	2.59 ± 0.23
NaturalL2S	3.54 ± 0.32	3.43 ± 0.27	3.21 ± 0.21
V2SFLow	3.88 ± 0.25	3.69 ± 0.25	3.90 ± 0.14
Proposed	4.17 ± 0.24	3.65 ± 0.25	3.77 ± 0.15

Table 2: MOS results on LRS3 dataset.

align the temporal resolution mismatch between the video and the audio, we upsample the visual features by using a transposed convolution layer.

The architecture of our SLD-L2S model is configured as follows. The subspace decomposition module partitions the 1024-dimensional visual features into 8 subspaces. Each subspace, containing a layer normalization and a 1D convolution, processes the features before they are concatenated. The backbone is composed of 12 DiCBs. Within each DiCB, the convolutional attention module employs a kernel of size (5, 7) for the time and subspace dimensions, respectively. The convolutional feedforward module uses a kernel size of 3 and expands the channel dimension to 1024. Conditional inputs are integrated via AdaLN-SOLA module, with the low-rank adjustment matrix rank set to 32. Finally, the subspace recomposition module projects the output from each of the 8 subspace streams to a dimension of 128. These are then concatenated and fused into a single 1024-dimensional vector. This fused representation is passed through ConvNeXt blocks, which consists of 3 layers with 512 hidden channels to facilitate final cross-channel interactions before producing the output. For training, we use the AdamW optimizer initialized with a learning rate of 2e-4 and the cosine learning rate decay strategy. The batch size is set to 16, and the model is trained for 150K iterations on a single NVIDIA H100 GPU over about five days. The AdamW scheme is configured with $\beta_1 = 0.8$, $\beta_2 = 0.99$. The hyperparameters for the auxiliary losses are set to $\lambda_1 = 1$ and $\lambda_2 = 100$.

Evaluation Metrics

We perform a comprehensive evaluation of our proposed SLD-L2S framework using a suite of objective and subjective metrics. The evaluation is designed to assess three critical aspects of the synthesized speech: perceptual quality, content intelligibility, and speaker similarity. For objective evaluation, we employ the following metrics:

□ **Quality:** We assess perceptual quality using UTMOS (Saeki et al. 2022) and SCOREQ (Ragano, Skoglund, and Hines 2024). Both are non-intrusive, reference-free models that predict a mean opinion score (MOS) on a 1-to-5 scale, designed to correlate with human quality judgments.

□ **Intelligibility:** We measure intelligibility from two perspectives. First, the word error rate (WER) is calculated using the AUTO-AVSR (Ma et al. 2023). Second, we utilize SpeechBERTScore (D-BERT) (Saeki et al. 2024), which leverages NLP evaluation metrics. It calculates the cosine similarity between the SSL embeddings of the synthesized

Method	UTMOS↑	SCOREQ↑	D-BERT↑	WER↓	SECS↑
Ours	4.2096	4.6075	0.8284	30.22	0.804
w/o DiCB	4.0835	4.5056	0.8184	30.70	0.618
w/o Repara	3.9540	4.2600	0.8249	29.70	0.809
w/o L_{sem}	4.1859	4.5830	0.8272	30.21	0.795
w/o L_{SLM}	4.2885	4.6958	0.8207	29.99	0.776
w/o L_{sem}	4.2507	4.6494	0.8157	30.53	0.771

Table 3: Ablation study results on the LRS3 dataset. Repara indicates the inclusion of our reparameterized flow matching object. DiCB signifies the replacement of our proposed DiCB backbone with DiT, maintaining closely matched parameter sizes (DiCB: 57.7M, DiT: 57.8M).

and target speech, providing a semantic similarity score in the range of -1 to 1.

□ **Speaker Similarity:** We quantify speaker identity preservation using speaker embedding cosine similarity (SECS). This metric is calculated from speaker embeddings, which are extracted from both the synthesized and target speech using the Resemblyzer (Wan et al. 2018) library.

Subjective evaluation is conducted through a MOS test. A group of 15 participants listened to 30 synthesized samples and were asked to rate each clip on three criteria: naturalness (how natural the speech sounds), intelligibility (how easy the content is to understand), and speaker similarity (how similar the synthesized speech is to the target speaker). All criteria were rated with 5 points (from 1 to 5).

Results and Discussion

Comparison with State-of-the-Art Methods

We compare our proposed SLD-L2S framework against advanced L2S methods: Intelligible (Choi, Kim, and Ro 2023), DiffV2S (Choi, Hong, and Ro 2023), LipVoicer (Yemini et al. 2023), NaturalL2S (Liang et al. 2025a), and V2SFLow (Choi et al. 2025). The results on the LRS3 and LRS2 datasets are presented in Table 1. Our analysis focuses on key aspects including perceptual quality, efficiency, intelligibility and speaker similarity. Notably, the LRS2 dataset is not used during training in order to evaluate the robustness.

First, the results unequivocally establish SLD-L2S as the new state-of-the-art in perceptual quality. As shown in Table 1, our model substantially outperforms all baselines on both datasets in the reference-free quality metrics. On the primary LRS3-TED benchmark, for instance, SLD-L2S surpasses the strongest flow matching based competitor, V2SFLow, by a margin of 0.5157 in UTMOS. Crucially, this superior synthesis quality is achieved with exceptional computational efficiency. SLD-L2S requires only 10 number of function evaluations (NFE) at inference, representing higher efficiency than other diffusion-based methods.

In terms of intelligibility, LipVoicer achieves the lowest WER because its reliance on a powerful, pre-trained visual speech recognition (VSR) model (Ma et al. 2023) to extract semantic features. However, this comes at the cost of degraded speech quality, as indicated by its low UTMOS and SCOREQ scores. Moreover, the require of a VSR model

Kernel size	UTMOS↑	SCOREQ↑	D-BERT↑	WER↓	SECS↑
Ours (5×7)	4.2096	4.6075	0.8284	30.22	0.804
3×5	4.2120	4.6016	0.8292	30.34	0.801
7×9	4.1914	4.5733	0.8291	30.17	0.800
9×11	4.2008	4.5852	0.8288	30.10	0.803

Table 4: Ablation study results of different kernel size on the LRS3 dataset. The kernel size is denoted as (time × subspace).

limits its applicability to scenarios where text transcripts are unavailable. In contrast, SLD-L2S strikes a superior balance. It generates intelligible speech, evidenced by its competitive D-BERT scores, which outperforms nearly all the methods without using specialized VSR front-ends and is highly competitive with the top performer, V2SFlow. This indicates that our model effectively generates intelligible speech while simultaneously preserving its perceptual quality.

For speaker identity preservation, V2SFlow achieves the highest SECS score as its training objective explicitly includes a speaker embedding loss to enforce speaker similarity. Despite not employing such a direct loss, our framework achieves a highly competitive second-best SECS score. This result underscores the effectiveness of our proposed DiCB module in conditioning the generation process on the speaker identity without requiring direct supervision.

The results of subjective evaluation, presented in Table 2, further validate the effectiveness of our framework. Our model excels in naturalness, achieving an outstanding score of 4.17 that notably surpasses all competitors and closely approaches the ground truth. In terms of intelligibility, our method ranks second with a score of 3.65. Focusing on speaker similarity, our model obtains a highly competitive score of 3.77, nearly matching the top-performing V2SFlow. This evaluation also highlights the limitations of relying solely on objective metrics. For instance, LipVoicer performs well on the objective WER metric but scores poorly in subjective tests, indicating that its poor acoustic quality and unnaturalness can severely degrade the practical intelligibility for human listeners. This discrepancy underscores that perceptual quality is a critical goal for L2S systems, as it directly impacts the ability of humans to comfortably understand the generated speech.

Ablation Study

To analyze the contribution of each component, we conduct an ablation study with results presented in Table 3.

□ **DiCB Architecture:** Replacing our DiCB backbone with a parameter-matched DiT leads to a significant performance collapse across nearly all metrics. This result underscores the critical role of our DiCB design in achieving high-quality synthesis and effective speaker conditioning.

□ **Reparameterized Training Objective:** Reverting to the standard velocity-prediction flow matching objective results in a notable drop in perceptual quality (UTMOS, SCOREQ). This confirms that our reparameterized approach is crucial for improving training stability and synthesis quality.

Subspaces	UTMOS↑	SCOREQ↑	D-BERT↑	WER↓	SECS↑
Ours (8)	4.2096	4.6075	0.8284	30.22	0.804
4	4.1797	4.5638	0.8278	29.94	0.802
16	4.1752	4.5683	0.8295	29.92	0.802
32	4.1288	4.5219	0.8268	30.35	0.799

Table 5: Ablation study results of different number of subspaces on the LRS3 dataset.

□ **Auxiliary Losses:** Removing the semantic loss (w/o \mathcal{L}_{sem}) causes a minor drop in quality and speaker similarity, suggesting its role as a helpful regularizer for the latent space. More interestingly, removing the SLM loss (w/o \mathcal{L}_{SLM}) reveals a trade-off: while this slightly improves the acoustic quality metrics (UTMOS/SCOREQ), it degrades both intelligibility (D-BERT) and speaker similarity (SECS). This indicates that the SLM loss is crucial for content and identity preservation, even if it introduces a slight constraint on the acoustic non-intrusive metrics. Removing both losses leads to a more pronounced degradation, confirming their combined importance.

Analysis on the design choices of DiCB

We further ablate two key design choices for our DiCB module: the convolutional kernel size and the number of subspaces. The results are summarized below.

□ **Kernel Size.** As shown in Table 4, model performance is remarkably robust to the kernel size in the convolutional attention module in DiCB. In contrast to the trend of using large kernels in computer vision, smaller kernels perform competitively in our task. The 5×7 kernel yields the best balance across all metrics, validating our choice.

□ **Number of Subspaces.** This proves to be a more sensitive hyperparameter. Table 5 reveals a distinct performance peak at our chosen configuration of 8 subspaces. Using fewer (4) or more (16, 32) subspaces leads to a marked degradation in perceptual quality (UTMOS/SCOREQ). This suggests that 8 subspaces achieve an optimal trade-off, effectively decomposing visual features without creating overly fragmented representations that are difficult to integrate.

Conclusion

In this paper, we introduced SLD-L2S, a novel framework that sets a state-of-the-art in lip-to-speech synthesis by directly mapping visual features to the latent space of audio codec. Our method leverages an efficient, reparameterized flow matching technique to train a hierarchical subspace network. This network is built upon our proposed diffusion convolution block, which effectively captures the intricate relationships between visual and auditory modalities. Combined with a dual semantic and SLM loss strategy for enhanced content fidelity, SLD-L2S notably surpasses existing methods in perceptual quality. Our work validates the potential of latent diffusion in lip-to-speech synthesis and provides a robust blueprint for the future of high-fidelity L2S synthesis.

References

Afouras, T.; Chung, J. S.; and Zisserman, A. 2018. LRS3-TED: a large-scale dataset for visual speech recognition. *arXiv preprint arXiv:1809.00496*.

Chen, S.; Wang, C.; Chen, Z.; Wu, Y.; Liu, S.; Chen, Z.; Li, J.; Kanda, N.; Yoshioka, T.; Xiao, X.; et al. 2022. Wavlm: Large-scale self-supervised pre-training for full stack speech processing. *IEEE Journal of Selected Topics in Signal Processing*, 16(6): 1505–1518.

Chen, Y.; Niu, Z.; Ma, Z.; Deng, K.; Wang, C.; Zhao, J.; Yu, K.; and Chen, X. 2024. F5-tts: A fairytaler that fakes fluent and faithful speech with flow matching. *arXiv preprint arXiv:2410.06885*.

Choi, J.; Hong, J.; and Ro, Y. M. 2023. DiffV2S: Diffusion-Based Video-to-Speech Synthesis with Vision-Guided Speaker Embedding. In *Proceedings of the IEEE/CVF International Conference on Computer Vision*, 7812–7821.

Choi, J.; Kim, J.-H.; Li, J.; Chung, J. S.; and Liu, S. 2025. V2sflow: Video-to-speech generation with speech decomposition and rectified flow. In *ICASSP 2025-2025 IEEE International Conference on Acoustics, Speech and Signal Processing (ICASSP)*, 1–5. IEEE.

Choi, J.; Kim, M.; and Ro, Y. M. 2023. Intelligible Lip-to-Speech Synthesis with Speech Units. In *INTERSPEECH 2023*, 4349–4353. ISCA.

Chung, J. S.; Nagrani, A.; and Zisserman, A. 2018. Voxceleb2: Deep speaker recognition. *arXiv preprint arXiv:1806.05622*.

Chung, J. S.; Senior, A.; Vinyals, O.; and Zisserman, A. 2017. Lip Reading Sentences in the Wild. In *IEEE Conference on Computer Vision and Pattern Recognition*.

Cooke, M.; Barker, J.; Cunningham, S.; and Shao, X. 2006. An audio-visual corpus for speech perception and automatic speech recognition. *The Journal of the Acoustical Society of America*, 120(5): 2421–2424.

Défossez, A.; Copet, J.; Synnaeve, G.; and Adi, Y. 2022. High fidelity neural audio compression. *arXiv preprint arXiv:2210.13438*.

Du, Z.; Chen, Q.; Zhang, S.; Hu, K.; Lu, H.; Yang, Y.; Hu, H.; Zheng, S.; Gu, Y.; Ma, Z.; et al. 2024. Cosyvoice: A scalable multilingual zero-shot text-to-speech synthesizer based on supervised semantic tokens. *arXiv preprint arXiv:2407.05407*.

Esser, P.; Kulal, S.; Blattmann, A.; Entezari, R.; Müller, J.; Saini, H.; Levi, Y.; Lorenz, D.; Sauer, A.; Boesel, F.; et al. 2024. Scaling rectified flow transformers for high-resolution image synthesis. In *Forty-first international conference on machine learning*.

Fu, Y.; Yan, Q.; Wang, L.; Li, K.; and Liao, R. 2025. Moflow: One-step flow matching for human trajectory forecasting via implicit maximum likelihood estimation based distillation. In *Proceedings of the Computer Vision and Pattern Recognition Conference*, 17282–17293.

Hai, J.; Xu, Y.; Zhang, H.; Li, C.; Wang, H.; Elhilali, M.; and Yu, D. 2024. Ezaudio: Enhancing text-to-audio generation with efficient diffusion transformer. *arXiv preprint arXiv:2409.10819*.

Harte, N.; and Gillen, E. 2015. TCD-TIMIT: An audio-visual corpus of continuous speech. *IEEE Transactions on Multimedia*, 17(5): 603–615.

Ho, J.; Jain, A.; and Abbeel, P. 2020. Denoising diffusion probabilistic models. *Advances in neural information processing systems*, 33: 6840–6851.

Hou, Q.; Lu, C.-Z.; Cheng, M.-M.; and Feng, J. 2024. Conv2former: A simple transformer-style convnet for visual recognition. *IEEE transactions on pattern analysis and machine intelligence*, 46(12): 8274–8283.

Hsu, W.-N.; Bolte, B.; Tsai, Y.-H. H.; Lakhota, K.; Salakhutdinov, R.; and Mohamed, A. 2021. Hubert: Self-supervised speech representation learning by masked prediction of hidden units. *IEEE/ACM Transactions on Audio, Speech, and Language Processing*, 29: 3451–3460.

Hsu, W.-N.; Remez, T.; Shi, B.; Donley, J.; and Adi, Y. 2023. ReVISE: Self-Supervised Speech Resynthesis With Visual Input for Universal and Generalized Speech Regeneration. In *Proceedings of the IEEE/CVF Conference on Computer Vision and Pattern Recognition*, 18795–18805.

Kim, J.-H.; Choi, J.; Kim, J.; Jung, C.; and Chung, J. S. 2025. From faces to voices: Learning hierarchical representations for high-quality video-to-speech. In *Proceedings of the Computer Vision and Pattern Recognition Conference*, 15874–15884.

Kim, J.-H.; Kim, J.; and Chung, J. S. 2024. Let there be sound: Reconstructing high quality speech from silent videos. In *Proceedings of the AAAI Conference on Artificial Intelligence*, volume 38, 2759–2767.

King, D. E. 2009. Dlib-ml: A machine learning toolkit. *The Journal of Machine Learning Research*, 10: 1755–1758.

Kumar, R.; Seetharaman, P.; Luebs, A.; Kumar, I.; and Kumar, K. 2023. High-fidelity audio compression with improved rvqgan. *Advances in Neural Information Processing Systems*, 36: 27980–27993.

Lei, S.; Cheng, X.; Lyu, M.; Hu, J.; Tan, J.; Liu, R.; Xiong, L.; Jin, T.; Li, X.; and Zhao, Z. 2024. Uni-dubbing: Zero-shot speech synthesis from visual articulation. In *Proceedings of the 62nd Annual Meeting of the Association for Computational Linguistics (Volume 1: Long Papers)*, 10082–10099.

Liang, Y.; Liu, F.; Li, A.; Li, X.; and Zheng, C. 2025a. NaturalL2S: End-to-End High-quality Multispeaker Lip-to-Speech Synthesis with Differential Digital Signal Processing. *arXiv preprint arXiv:2502.12002*.

Liang, Y.; Yang, K.; Liu, F.; Li, A.; Li, X.; and Zheng, C. 2025b. LightL2S: Ultra-Low Complexity Lip-to-Speech Synthesis for Multi-Speaker Scenarios. In *Proc. Interspeech 2025*, 3783–3787.

Lipman, Y.; Chen, R. T.; Ben-Hamu, H.; Nickel, M.; and Le, M. 2022. Flow matching for generative modeling. *arXiv preprint arXiv:2210.02747*.

Liu, Z.; Mao, H.; Wu, C.-Y.; Feichtenhofer, C.; Darrell, T.; and Xie, S. 2022. A convnet for the 2020s. In *Proceedings of the IEEE/CVF conference on computer vision and pattern recognition*, 11976–11986.

Ma, P.; Haliassos, A.; Fernandez-Lopez, A.; Chen, H.; Petridis, S.; and Pantic, M. 2023. Auto-avsr: Audio-visual speech recognition with automatic labels. In *ICASSP 2023-2023 IEEE International Conference on Acoustics, Speech and Signal Processing (ICASSP)*, 1–5. IEEE.

Milner, B.; and Le Cornu, T. 2015. Reconstructing Intelligible Audio Speech from Visual Speech Features. In *Inter-speech 2015*.

Peebles, W.; and Xie, S. 2023. Scalable diffusion models with transformers. In *Proceedings of the IEEE/CVF international conference on computer vision*, 4195–4205.

Polyak, A.; Adi, Y.; Copet, J.; Kharitonov, E.; Lakhota, K.; Hsu, W.-N.; Mohamed, A.; and Dupoux, E. 2021. Speech resynthesis from discrete disentangled self-supervised representations. *arXiv preprint arXiv:2104.00355*.

Prajwal, K.; Mukhopadhyay, R.; Namboodiri, V. P.; and Jawahar, C. 2020. Learning individual speaking styles for accurate lip to speech synthesis. In *Proceedings of the IEEE/CVF conference on computer vision and pattern recognition*, 13796–13805.

Ragano, A.; Skoglund, J.; and Hines, A. 2024. SCOREQ: Speech quality assessment with contrastive regression. *Advances in Neural Information Processing Systems*, 37: 105702–105729.

Ren, Y.; Hu, C.; Tan, X.; Qin, T.; Zhao, S.; Zhao, Z.; and Liu, T.-Y. 2020. Fastspeech 2: Fast and high-quality end-to-end text to speech. *arXiv preprint arXiv:2006.04558*.

Saeki, T.; Maiti, S.; Takamichi, S.; Watanabe, S.; and Saruwatari, H. 2024. Speechbertscore: Reference-aware automatic evaluation of speech generation leveraging nlp evaluation metrics. *arXiv preprint arXiv:2401.16812*.

Saeki, T.; Xin, D.; Nakata, W.; Koriyama, T.; Takamichi, S.; and Saruwatari, H. 2022. Utmos: Utokyo-sarulab system for voicemos challenge 2022. *arXiv preprint arXiv:2204.02152*.

Shen, K.; Ju, Z.; Tan, X.; Liu, Y.; Leng, Y.; He, L.; Qin, T.; Zhao, S.; and Bian, J. 2023. Naturalspeech 2: Latent diffusion models are natural and zero-shot speech and singing synthesizers. *arXiv preprint arXiv:2304.09116*.

Shi, B.; Hsu, W.-N.; Lakhota, K.; and Mohamed, A. 2022. Learning audio-visual speech representation by masked multimodal cluster prediction. *arXiv preprint arXiv:2201.02184*.

Wan, L.; Wang, Q.; Papir, A.; and Moreno, I. L. 2018. Generalized end-to-end loss for speaker verification. In *2018 IEEE International Conference on Acoustics, Speech and Signal Processing (ICASSP)*, 4879–4883. IEEE.

Wang, C.; Chen, S.; Wu, Y.; Zhang, Z.; Zhou, L.; Liu, S.; Chen, Z.; Liu, Y.; Wang, H.; Li, J.; et al. 2023. Neural codec language models are zero-shot text to speech synthesizers. *arXiv preprint arXiv:2301.02111*.

Wang, Y.; and Zhao, Z. 2022. FastLTS: Non-Autoregressive End-to-End Unconstrained Lip-to-Speech Synthesis. In *Proceedings of the 30th ACM International Conference on Multimedia*, MM ’22, 5678–5687. Association for Computing Machinery. ISBN 978-1-4503-9203-7.

Yang, D.; Liu, S.; Huang, R.; Tian, J.; Weng, C.; and Zou, Y. 2023. Hifi-codec: Group-residual vector quantization for high fidelity audio codec. *arXiv preprint arXiv:2305.02765*.

Ye, Z.; Sun, P.; Lei, J.; Lin, H.; Tan, X.; Dai, Z.; Kong, Q.; Chen, J.; Pan, J.; Liu, Q.; et al. 2025. Codec does matter: Exploring the semantic shortcoming of codec for audio language model. In *Proceedings of the AAAI Conference on Artificial Intelligence*, volume 39, 25697–25705.

Yemini, Y.; Shamsian, A.; Bracha, L.; Gannot, S.; and Fetaya, E. 2023. Lipvoicer: Generating speech from silent videos guided by lip reading. *arXiv preprint arXiv:2306.03258*.

Zeghidour, N.; Luebs, A.; Omran, A.; Skoglund, J.; and Tagliasacchi, M. 2021. Soundstream: An end-to-end neural audio codec. *IEEE/ACM Transactions on Audio, Speech, and Language Processing*, 30: 495–507.

Zheng, Z.; Peng, X.; Yang, T.; Shen, C.; Li, S.; Liu, H.; Zhou, Y.; Li, T.; and You, Y. 2024. Open-sora: Democratizing efficient video production for all. *arXiv preprint arXiv:2412.20404*.